Vision based Multi-rate Estimation and Control of Body Slip Angle for Electric Vehicles

Yafei Wang*, BinhMinh Nguyen*, Hiroshi Fujimoto**, and Yoichi Hori**
*Department of Electrical Engineering, The University of Tokyo, Tokyo, 113-8656, Japan
**Department of Advanced Energy, The University of Tokyo, Chiba, 153-8505, Japan
E-mail :{wang, minh}@hori.k.u-tokyo.ac.jp, {fujimoto, hori}@k.u-tokyo.ac.jp

***Abstract*-Among many vehicle states, body slip angle is one of the most important information for vehicle motion control. Due to the high costs to measure body slip angle with specific devices, it is necessary to investigate estimation methods using existing cheap sensors. From the viewpoint of sensor configuration, gyroscope, steering angle sensor, etc. are often employed for body slip angle estimation; in this research, two pieces of information provided by vision system are also utilized as additional measurements. Nevertheless, the sampling rate of normal camera is much slower compared to the other kinds of onboard sensors; for electric vehicles (EVs), motors' control period is shorter than the sampling time of cameras, which also brings multi-rate issue. Moreover, the time delay caused by image processing is usually too long to be neglected. In this paper, single-rate and multi-rate Kalman filters considering measurement delay are designed for body slip angle estimation, and a body slip angle controller is designed with the estimated result as feedback. First of all, vehicle model and visual model as well as the multi-rate and delay issues are explained; then, single-rate and multi-rate Kalman filters are designed for body slip angle estimation; and then, body slip angle controllers with single-rate and multi-rate estimators are compared followed with simulations and experimental results; finally, conclusion and future works are presented.**

I. INTRODUCTION

For vehicle motion control systems, body slip angle is known to be one of the key enablers. However, existing products such as optical sensor are too expensive to be practically employed [1-2]. Therefore, methods for vehicle body slip angle estimation have been extensively studied during the last few decades, and most of them employ bicycle-model-based observers [2-3]. However, bicycle model contains uncertainties and the estimation results are affected by them. On the other hand, visual model is purely based on simple geometry and contains much fewer uncertainties compared with vehicle model [4]. Moreover, vision system can give accurate position measurements for lane keeping [5]. If body slip angle estimator adopts visual information, the estimated results can be more robust against model errors accordingly. However, due to vision system's low throughput characteristic and the delay caused by image processing, they are seldom utilized for vehicle motion control related applications. For EVs, in particular, the frequency of control input can be as fast as 1 kHz [13]. If the updating rate of vision system can be boosted, information from cameras can be adopted for EV motion control.

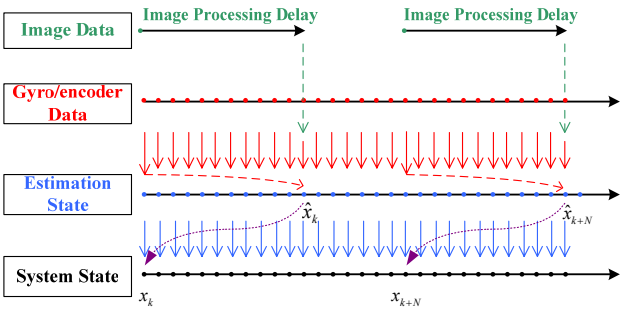

Fig. 1. System time sequence diagram.

Based on the above stated background, in this research, traditional bicycle model is augmented with a visual model, and the new system has four states with three of them available from sensor or image processing program, and body slip angle is the only state needs to be estimated. Bicycle model uses signals from gyroscope and encoders; visual model utilizes information calculated from onboard vision system. As can be seen from the time sequence diagram in Fig.1, the sampling times of gyro sensor and encoders are synchronized with system states (1 ms in this application); the sampling time of vision system is 33 ms and the data are delayed for 33 ms due to image processing time. Obviously, data from vision system and from gyro/encoders cannot be fused directly because of sampling discrepancy. To solve this multi-rate issue, two solutions can be employed, namely, single-rate-based method and multi-rate-based method. Single-rate estimator reduces the overall sampling rate to fit the slowest device, and the overall sampling time is increased accordingly. For multi-rate estimator, by estimating inter-sample residuals, system states can be updated every 1 ms. For time delay, lifting method is applied in this research [14]. After obtaining desired vehicle state, a two-degree-of-freedom controller is constructed with the estimated result (single-rate-based or multi-rate-based) as feedback. Considering controller performance, the system open loop stability margin can be increased with faster feedback [16].

II. PROBLEM STATEMENT

A. *Modeling of Vehicle and Vision System*

Vehicle bicycle model is widely used in vehicle state estimation and control systems; for vehicles with IWMs, differential torque generated by left and right wheels should be also considered into the model. This model is illustrated in

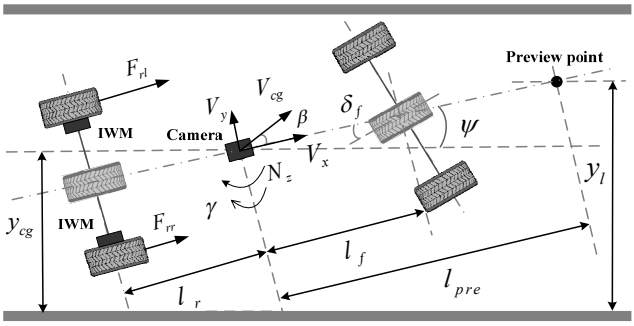

Fig. 2. Combined vehicle and vision model.

Fig. 2, and the governing equations can be found in [2, 15]. β is body slip angle at vehicle's CoG (center of gravity), γ is yaw rate, δ_f is steering angle, V_x is vehicle longitudinal speed, m is vehicle mass, N_z is yaw moment generated by differential torque of rear wheels, I is moment of inertial about yaw axis, C_f and C_r are cornering stiffness of the front and rear wheels respectively, l_f and l_r are distance front CoG to front and rear wheels respectively.

Vision model is also shown in Fig. 2, and the gray borders are lane makers on the road. In this model, it is assumed that the vehicle travels along a straight road with clear lane markers and the on-board camera can detect lane boundaries in real time. The lane function is obtained in the coordinate system with camera as origin; and then, lateral offset y_l at a preview point, as well as the heading angle ψ can be calculated. y_{cg} is the lateral offset at CoG, l_{pre} is a fixed preview distance needs to be calibrated beforehand. The equations can then be derived based on geometry [15].

Combining the vehicle and vision models, a new model can be given in continuous state space form as (1), where w and v are the process and measurement noises respectively.

$$\dot{x} = A \cdot x + B \cdot u + w$$
$$y = C \cdot x + v \tag{1}$$

where

$$x = \begin{bmatrix} \beta & \gamma & \psi & y_l \end{bmatrix}^T, \quad u = \begin{bmatrix} \delta_f & N_z \end{bmatrix}^T, \quad y = \begin{bmatrix} \gamma & \psi & y_l \end{bmatrix}^T,$$

$$A = \begin{bmatrix} -\frac{2(c_f + c_r)}{m V_x} & -1 - \frac{2(c_f l_f - c_r l_r)}{m V_x^2} & 0 & 0 \\ -\frac{2(c_f l_f - c_r l_r)}{I} & -\frac{2(c_f l_f^2 + c_r l_r^2)}{I V_x} & 0 & 0 \\ 0 & 1 & 0 & 0 \\ V_x & l_{pre} & V_x & 0 \end{bmatrix},$$

$$B = \begin{bmatrix} \frac{2c_f}{m V_x} & \frac{2c_f l_f}{I} & 0 & 0 \\ 0 & \frac{1}{I} & 0 & 0 \end{bmatrix}^T, \quad C = \begin{bmatrix} 0 & 1 & 0 & 0 \\ 0 & 0 & 1 & 0 \\ 0 & 0 & 0 & 1 \end{bmatrix}.$$

B. Multi-rate and delayed measurements

To estimate body slip angle β, a discretized Kalman filter is designed in (2) based on (1). T_s is the sampling time of the system. As vehicle speed is not constant, the state space matrices are time varying.

$$x(k+1) = A_d(k) \cdot x(k) + B_d(k) \cdot u(k) + w(k)$$
$$y(k) = C_d(k) \cdot x(k) + v(k) \tag{2}$$

where

$$A_d(k) = e^{A \cdot Ts}, \quad B_d(k) = \int_0^{Ts} e^{A \cdot \tau} \cdot B d\tau,$$
$$C_d(k) = C.$$

In the combined vehicle and vision model, it should be noticed that there are two measurement times: longer sampling time is defined as T_c, and shorter sampling time is defined as T_s. Therefore, the selection of T_s and T_c for system discretization needs to be considered. If sampling time is set to be the longer one, data from fast sensor have to be dropped between inter-samples of the slow speed sensor. This can easily solve the multi-rate issue, but obviously deteriorates estimation performance. An alternative solution is to set system sampling time to the shorter one and estimate inter-sample residuals for the slow-rate measurements.

Moreover, the measurements from vision system are delayed due to image processing. In fact, image processing time varies due to incoming images and hardware processing loads. In this research, for the convenience of post-processing, a constant image processing time is implemented in the program as described later in this paper. Therefore, the visual outputs equation becomes (3), where T_d is the time delay, $n_d = T_d/T_s$. Here, $T_d = T_c = 33$ ms, and $T_s = 1$ ms.

$$y(k) = C_d(k - n_d) \cdot x(k - n_d) + v(k - n_d) \tag{3}$$

From (3), it is known that, unlike normal measurements, the information from visual system is captured at step k-n_d, but is not available until step k. The whole system output equation therefore has the form of (4). Here, two interpretations can be made for the delays: a) visual information is delayed n_d times with fast data as reference; b) visual information is delayed one time with itself as reference. As the multi-rate ratio between fast and slow sensors is generally high, it is desirable to consider the delay using interpretation b) that can simplify estimator design.

$$y(k) = \begin{bmatrix} C_d^{veh}(k) & O \\ O & C_d^{vis}(k - n_d) \end{bmatrix} \cdot \begin{bmatrix} x^{veh}(k) \\ x^{vis}(k - n_d) \end{bmatrix} + \begin{bmatrix} v^{veh}(k) \\ v^{vis}(k - n_d) \end{bmatrix} \tag{4}$$

III. BODY SLIP ANGLE ESTIMATION AND CONTROL

In this section, body slip angle observer is designed based on the combined vehicle/vision model using both single-rate and multi-rate Kalman filters; body slip angle controller is then designed with estimated β as feedback.

A. Body Slip Angle Estimation with Combined Vehicle and Vision Model

As stated in section II, there are two issues for estimator design, namely, delayed and multi-rate measurements. Before considering the multi-rate issue, time delay has to be solved first. Lifting method is employed to deal with the measurement delay, and the basic idea is to include delayed states into the state space equation [14].

First, considering information from vision system has a one step delay, (5) is defined:

$$\bar{\psi}(k+1)=\psi(k),\quad \bar{y}_l(k+1)=y_l(k) \tag{5}$$

Then, the discretized state space equation, (2), is augmented with (5) as additional states, and (6) gives description for the new system.

With the above transformation, delayed visual information is augmented to the original system. As this system is observable, current visual states can be estimated with Kalman filter based on the information one step before. Then, to solve the multi-rate issue, two solutions are adopted here, namely, single-rate and multi-rate Kalman filters.

$$x^a(k)=[\beta(k)\quad \gamma(k)\quad \psi(k)\quad y_l(k)\quad \bar{\psi}(k)\quad \bar{y}_l(k)]^T,$$

$$u(k)=[\delta_f(k)\quad N_z(k)],\ y^a(k)=[\gamma(k)\quad \bar{\psi}(k)\quad \bar{y}_l(k)]^T,$$

$$A_d^a(k)=\begin{bmatrix} A_d(k) & O_{4\times 2} \\ O_{2\times 2} & I_{2\times 2}\quad O_{2\times 2}\end{bmatrix},\ B_d^a(k)=[B_d(k)\quad 0\quad 0]^T,$$

$$C_d^a(k)=C_d^a=\begin{bmatrix}0&1&0&0&0&0\\0&0&0&0&1&0\\0&0&0&0&0&1\end{bmatrix}. \tag{6}$$

1) Single-rate Kalman filter design

Single-rate Kalman filter simply adapt the sampling rate of high speed sensor to the slow speed device. In this study, to unify the sampling rate of gyroscope, encoders and camera, system sampling rate is set to adapt camera. The data from fast sensors are ignored during inter-samples. The measurement of single-rate Kalman filter can then be constructed as (7).

$$\hat{x}^a(k+1\,|\,k+1)=\hat{x}^a(k+1\,|\,k)+K(k+1)\cdot[y(k+1)-C_d^a\cdot\hat{x}^a(k+1\,|\,k)]$$
$$\text{... only when } k+1=n\cdot(T_C/T_S) \tag{7}$$

Although traditional Kalman filter can be employed by making the sampling rate adjustment, other problems are arisen, for example, measurements from high sampling rate sensors cannot be fully utilized and hence deteriorate the accuracy of sensor feedback; the estimated body slip angle is updated every 33 ms which is not fast enough for EV motion control [13].

2) Multi-rate Kalman filter design

Multi-rate Kalman filter first discretize the system using fast sampling time (here, T_s is set to 1 ms). Compared with single-rate Kalman filter, the time update of Multi-rate one is the same, and pseudo-corrections need to be implemented for slow rate sensors during inter-samples. Assume the camera's sampling period is T_c, and during the time intervals of $n\cdot T_c$ (n is an integer), there is no updates from vision system. Then, an intuitive solution is to assume the measurements from vision system are exactly the same with prediction, in other words, the visual residuals are set to zeros. By this way, between low-speed sensor's inter-samples, corrections can still be made with fast-speed sensors. In this application, the correction of Kalman filter is only based on yaw rate from gyro sensor during visual inter-sampling times.

The state estimation equation for multi-rate Kalman filter is shown in (8).

$$\hat{x}^a(k+1|k+1)=\hat{x}^a(k+1|k)+K(k+1)\cdot[\tilde{y}^a(k+1)-C_d^a\cdot\hat{x}^a(k+1|k)] \tag{8}$$

where

$$\tilde{y}^a(k+1)=\begin{cases}[\gamma(k+1),\tilde{\bar{\psi}}(k+1),\tilde{\bar{y}}_l(k+1)]^T, & \text{if } k+1\neq n\cdot(T_C/T_S),\\ [\gamma(k+1),\bar{\psi}(k+1),\bar{y}_l(k+1)]^T, & \text{if } k+1=n\cdot(T_C/T_S).\end{cases}$$

Although the above pseudo-measurement can perform better than the single-rate Kalman filter, it is necessary to investigate estimation convergence during inter-samples. For simplicity, only time-invariant system is considered here, and time-varying system can be studied in the same way.

Ideally, measurements can be feedback at every sample, and the observation error at step $k+n$ is given in (9), where K is the steady state Kalman gain. Obviously, the Kalman gain performs n times, and a suitable K can make observation error converges gradually.

$$e_{k+n}=x_{k+n}-\hat{x}_{k+n}$$
$$=[(I-K\cdot C)\cdot A]^n\cdot e_k+\sum_{i=1}^{n}[(I-K\cdot C)\cdot A]^{i-1}\cdot w \tag{9}$$

In case of no measurements during inter-samples, observation error becomes (10). It can be seen that the K only performs one time and e_{k+n} increases gradually. In this case, the final estimation result can not converge.

$$e_{k+n} = x_{k+n} - \hat{x}_{k+n} = A^{n-1}\left[(I - K \cdot C) \cdot A\right] \cdot e_k + \sum_{m=1}^{n-1} A^{m-1}\left[(I - K \cdot C) \cdot A\right] \cdot w \qquad (10)$$

For the application of combined vehicle and vision model, the estimation error depends on measurements from two sources. As the visual part can not converge, the convergence of the whole system is questionable. Therefore, the residuals during inter-samples should be computed for estimation convergence [8] and [17]. First of all, the residual at time k when there is measurement updates is given as (11).

$$\varepsilon_k = y_k - C \cdot \overline{x}_k = C \cdot (\overline{x}_k - x_k) + v \qquad (11)$$

Considering that C may not be invertible, (12) can be constructed from (11).

$$x_k = \overline{x}_k + (C^T \cdot C)^{-1} \cdot C^T \cdot (\varepsilon_k - v) \qquad (12)$$

From the definition of e_k as well as from (12), (13) can be obtained as below.

$$e_k = [(C^T \cdot C)^{-1} \cdot C^T - K] \cdot \varepsilon_k - (C^T \cdot C)^{-1} \cdot C^T \cdot v \qquad (13)$$

On the other hand, during inter-samples when there are no measurement updates, estimation error is given as (14).

$$\begin{aligned} e_{k+n} &= x_{k+n} - \hat{x}_{k+n} \\ &= x_{k+n} - \overline{x}_{k+n} - K \cdot (y_{k+n} - C \cdot \overline{x}_{k+n}) \\ &= (x_{k+n} - \overline{x}_{k+n}) - K \cdot (C \cdot x_{k+n} + v - C \cdot \overline{x}_{k+n}) \\ &= (I - K \cdot C) \cdot A \cdot e_{k+n-1} + (I - K \cdot C) \cdot w - K \cdot v \end{aligned} \qquad (14)$$

The pseudo-residual when measurements are not available can be given in (15), and it is updated with (14).

$$\begin{aligned} \varepsilon_{k+n} &= y_{k+n} - C \cdot \overline{x}_{k+n} \\ &= C \cdot x_{k+n} + v - C \cdot \overline{x}_{k+n} \\ &= C \cdot A \cdot e_{k+n-1} + C \cdot w + v \end{aligned} \qquad (15)$$

Finally, to check the convergence, estimation error in this case is represented by e_k in (16).

$$\begin{aligned} e_{k+n} &= x_{k+n} - \hat{x}_{k+n} \\ &= \left[(I - K \cdot C)A\right]^n + \sum_{i=0}^{n-1} [A \cdot (I - K \cdot C)]^i \cdot w \\ &\quad - \sum_{i=0}^{n-1} [(I - K \cdot C) \cdot A]^i \cdot K \cdot v \end{aligned} \qquad (16)$$

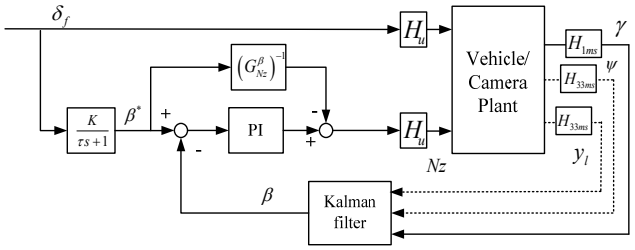

Fig. 3. Controller structure with body slip angle estimator.

From (16), it can be known that the first term is the same with the idea case, and the convergence can be guaranteed.

B. Controller Design for Vehicle Body Slip Angle

It is reported that drivers are sensitive to large body slip angle during driving [2]. Therefore, it is desirable to implement control system for driver assistance that can manipulate body slip angle to a desired value. In case of vehicles IWMs, the differential torque of left and right wheels can be employed as control input.

The overall control structure is shown in Fig. 3. The reference of body slip angle is generated as a function of steering angle, and is then passed to a two-degree-of-freedom controller to generate control input. For the feedback signal, body slip angle is estimated with both single-rate and multi-rate Kalman filters. It should be noticed that the control inputs have the sampling rate of 1 ms and the outputs are sampled at different rates. Single-rate Kalman filter generates 33 ms sampling rate and multi-rate Kalman filter outputs estimation result every 1 ms. Here, only body slip angle is controlled; actually, vehicle heading angle and lateral offset information with 1 ms updating rate can also be employed for lane keeping control [5].

IV. EXPERIMENTAL SETUPS

The experimental vehicle used in this research is named COMS as shown in Fig. 4. It is an EV produced by Toyota Auto Body, and was modified by our lab for motion control and capacitor related study [11].

The vehicle controller is a PC104 embedded computer with real-time Linux system, and the program is configured to run at the speed of one millisecond per cycle. In addition to the central computer, four A/D converters and two counter boards are equipped for sensor signal reading. Gyroscope is installed in the vehicle CoG, and provides yaw rate signal to the A/D board; steering angle and wheel speed encoders send data to the counter board. Besides, to verify estimation result, an optical β sensor is also equipped for body slip angle acquisition. Vision system includes a camera and an image processing laptop; the camera is Grasshopper produced by Point Grey, and the frame rate of the camera is set to 30 fps. Images captured by the camera are then processed by a laptop with image processing algorithm. The image processing time is set to constant (30 ms) by adding delays. The final outputs from vision system are the estimated ψ and y_l, and they are sent to vehicle controller via LAN cable using UDP protocol.

Fig. 4. Experimental vehicle COMS.

V. SIMULATIONS AND EXPERIMENTS

A. Simulations

First, simulations were conducted to verify the performance of single-rate and multi-rate Kalman filters. The vehicle was assumed to run at the speed of 30 km/h, and a sine steering input was given. To clearly demonstrate the effectiveness of the proposed method, vehicle and Kalman filter models were made different from each other: the cornering stiffness, C_f and C_r, as well as the mass of the vehicle plant were set 1.5 times and 2 times bigger than the estimator ones respectively. In Fig. 5, it can be observed that bicycle model-based Kalman filter can not converge to true value due to the model discrepancy; single-rate Kalman filter performs better due to the add of visual information; multi-rate Kalman filter with inter-sample estimation gives best result compared to the previous two methods.

Then, with both single-rate and multi-rate Kalman filters, the performances of body slip angle controller were compared in simulation. Due to the low stability margin, the feedback gain in case of single-rate Kalman filter can not be set to be large enough for reference tracking. On the other hand, the feedback gain in case of multi-rate Kalman filter can be set to a large value to track the reference, i.e., the stability margin is increased. The simulation results are demonstrated in Fig. 6.

B. Experiments

Similar to simulations, both estimation and control performances were verified in experiments. Experiments were conducted with the experimental vehicle introduced in the last section. The vehicle was given a sine steering input

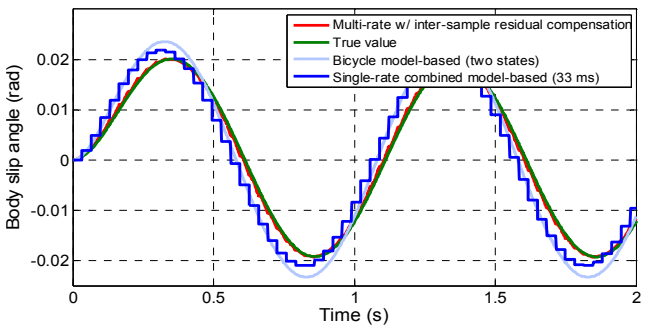

Fig. 5. Estimation results comparison.

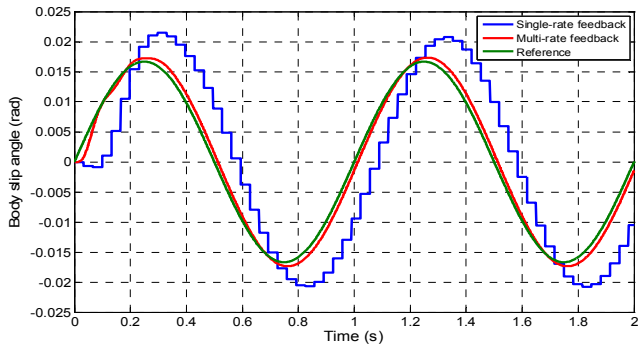

Fig. 6. Controller performance comparison.

on a road with lane markers, and the vehicle speed varied from 15 km/h to 25 km/h.

First, Kalman filters were implemented for body slip angle estimation. As the exact vehicle model is difficult to be obtained, models between Kalman filter and true vehicle are different. Fig. 7 gives comparison of bicycle model-based Kalman filter, combined model-based single-rate Kalman filter, and combined model-based multi-rate Kalman filter. Due to the model discrepancy, bicycle model-based result cannot track the true value very well. The combined model-based single-rate estimator's performance is also poor due to down-sampling. The multi-rate Kalman filter with inter-sample residual compensation performs much better than the other two methods.

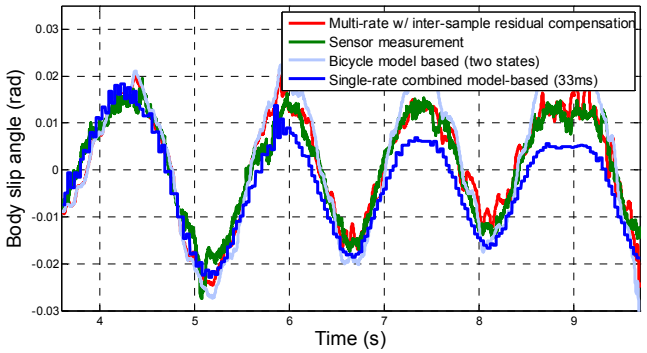

Fig. 7. Estimation method comparisons based on experimental data.

Then, with both single-rate and multi-rate Kalman filters, controllers were implemented in experiments. The vehicle was given a sine steering input, and IWMs were used to gene-

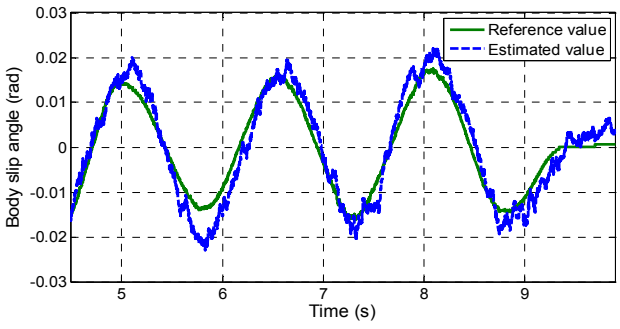

(a) Control performance with single-rate Kalman filter.

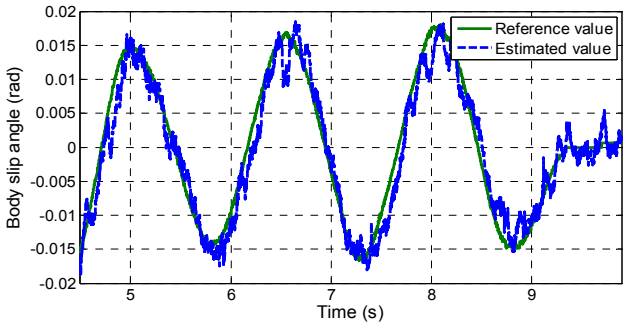

(b) Control performance with multi-rate Kalman filter.

Fig. 8. Body slip angle control performance comparison.

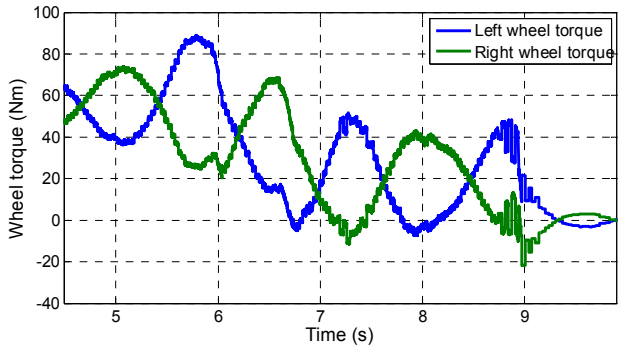

(a) single-rate feedback based.

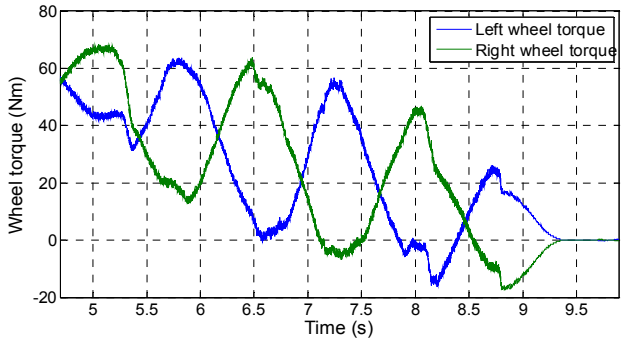

(b) multi-rate feedback based.

Fig. 9. Motor torque input comparison.

rate differential torque to control the vehicle body slip angle for reference tracking. In Fig. 8, the performance of controller with single-rate estimator-based feedback and multi-rate estimator-based feedback are compared. Fig. 9 gives the comparison of control input generated by IWMs.

VI. CONCLUSION AND FUTURE WORKS

In this paper, first of all, a combined vehicle and visual model was derived, and the multi-rate and delay issues were explained; then, single-rate Kalman filter which has low updating rate and multi-rate Kalman filters with inter-sample residual estimation that can be updated every 1 ms were designed to estimate vehicle body slip angle; then, body slip angle controller was designed with both single-rate and multi-rate estimators; finally, simulations and experiments were conducted to verify and compare the proposed estimators and controllers. Multi-rate Kalman filter can enhance system stability margin compared to the single-rate one. The further step of this research is to expand vision system to other vehicle motion estimation and control applications, for example, enhanced lane keeping control, roll angle estimation and control and so on.

REFERENCES

[1] Y. Hori, “Future Vehicle driven by Electricity and Control -Research on 4 Wheel Motored ‘UOT March II’,” IEEE Trans. Ind. Electron., vol.51, no.5, pp.954-962, Oct. 2004.

[2] C. Geng, L. Mostefai, M. Denai and Y. Hori, “Direct Yaw Moment Control of an In-Wheel-Motored Electric Vehicle Based on Body Slip Angle Fuzzy Observer,” IEEE Trans. Ind. Electron., vol.56, no.5, pp.1411-1419, May 2009.

[3] T. Hiraoka, H. Kumamoto, O. Nishihara, “Sideslip angle estimation and active front steering system based on lateral acceleration data at centers of percussion with respect to front/rear wheels,” JSAE Review, vol.25, no.1, pp.37-42, 2004.

[4] J. Hsu, M. Tomizuka, “Analyses of vision-based lateral control for automated highway system,” Vehicle system dynamics, Volume. 30, Issue. 5, pp. 345-373, 1998.

[5] Joel C. McCall and Mohan M. Trivedi, “Video Based Lane Estimation and Tracking for Driver Assistance: Survey, System, and Evaluation,” IEEE Trans. Intell. Transp. Syst., vol.7, pp.20-37, 2006.

[6] G. Bradski, A. Kaehler, “Learning OpenCV: Computer Vision with the OpenCV Library,” O'Reilly, Cambridge, MA, 2008.

[7] M. S. Grewal and A. P. Andrews, Kalman Filtering: Theory and Practice Using MATLAB, Wiley Online Library, 2001.

[8] S. On, and Y. Hori, “Development of a Novel Instantaneous Speed Observer and its Application to the Power-Assisted Wheelchair Control,” Proc. 4th International Conference on Power Electronics and Motion Control, Xi'an, China, 2004.

[9] L. Chu, Y. Zhang, M. Xu, Y. Shi, and O. Yang, “Design of a robust side slip angle observer using adaptive Kalman filter,” Computer Design and Applications (ICCDA), 2010 International Conf. on, 2010.

[10] M. Chen, T. Jochem, D. Pomerleau, “AURORA: A Vision-Based Roadway Departure Warning system,” Proceedings of IEEE International Conf. on Intelligent Robots and Systems, Pittsburgh, PA, August, 1995, pp. 243–248, 1995.

[11] K. Kawashima, T. Uchida, and Y. Hori, “Manufacturing of Small Electric Vehicle driven only by Electric Double Layer Capacitors for Easy Experiment of Vehicle Motion Control,” Electric Vehicle Symposium 21, 2005.4.

[12] M. Bertozzi and A. Broggi, “GOLD: a Parallel Real-Time Stereo Vision System for Generic Obstacle and Lane Detection,” IEEE Trans. Image Process, pp. 62-81, Jan. 1998.

[13] D. Yin, Y. Hori, “A Novel Traction Control for EV Based on Maximum Transmissible Torque Estimation,” IEEE Trans. Ind. Electron., vol. 56, no.6, 2009.

[14] S. Challa, R. Evans and X. Wang, “A Bayesian solution and its approximations to out-of-sequence measurement problems,” Journal of Information Fusion, vol. 4, issue 3, pp. 185-199, Sept. 2003.

[15] Y. Wang, P. Kotchapansompote, BM Nguyen, H. Fujimoto, and Y. Hori, "Vision-based vehicle body slip angle estimation with multi-rate Kalman filter considering time delay," Industrial Electronics (ISIE), 2012 IEEE International Symposium on, vol., no., pp.1506-1511, 28-31 May 2012.

[16] H. Fujimoto, Y. Hori, "Visual servoing based on multirate sampling control-application of perfect disturbance rejection control," In Proceedings 2001 ICRA. IEEE Int. Conf. on Robotics and Automation, vol. 1, pp. 711–716, 2001

[17] B. M. Nguyen, Y. Wang, H. Fujimoto, and Y. Hori, “Sideslip Angle Estimation Kalman Filter with Model Error and Disturbance Compensation for Electric Vehicle," 8th IEEE Vehicle Power and Propulsion Conference, 2012 (accepted).